

OVERCOMING MULTIPACTING BARRIERS IN SRF PHOTOINJECTORS

I. Petrushina¹, V. N. Litvinenko¹, G. Narayan, I. Pinayev, F. Severino, K. S. Smith
Brookhaven National Laboratory, Upton, Long Island, New York, USA
¹also at Stony Brook University, Stony Brook, Long Island, New York, USA

Abstract

Superconducting RF (SRF) photoinjectors are considered to be a potential breakthrough in the area of high brightness electron sources. However, there is always the very important question of the compatibility of SRF cavities and high quantum efficiency (QE) photocathodes. A deposition of active elements from high QE photocathodes on the surface of a cavity makes it more vulnerable to multipacting (MP) and could affect the operation of an SRF gun. On the other side, MP can significantly reduce the lifetime of a photocathode. It is well known in the SRF community that a strong coupling, high forward power and sufficient cleanliness of cavity walls are the key components to overcome a low-level MP zone. In this paper we present a theoretical model of passing a MP barrier which could help estimate the desirable conditions for successful operation of an SRF gun. We demonstrate our results for the 113 MHz SRF photo-injector for Coherent electron Cooling (CeC) alongside with the experimental observations and 3D simulations of the MP discharge in the cavity. The results of the theoretical model and simulations show good agreement with the experimental results, and demonstrate that, if approached carefully, MP zones can be easily passed without any harm to the photocathode.

CEC POP SRF PHOTOINJECTOR

The superconducting 113 MHz photoinjector is the essential part of the electron accelerator for the Coherent electron Cooling [1] Proof-of-Principal (CeC PoP) experiment at Brookhaven National Laboratory [2]. During the last couple of years, it has successfully delivered high-charge electron bunches with up to 10 nC per bunch, and demonstrated an excellent performance with the cathodes operating for months without significant loss of quantum efficiency [3].

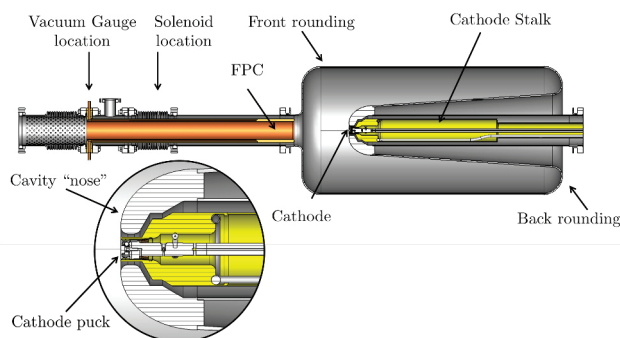


Figure 1: Simplified geometry of the CeC PoP SRF photo injector.

The gun is based on Quarter Wave Resonator (QWR) and operates at 1.25 MV of accelerating voltage. Figure 1

demonstrates the cross-section of the gun cavity and its major components: fundamental power coupler (FPC), cathode stalk and the cathode itself. The hollow FPC is located in the front of the cavity and allows for the propagation of the generated beam outside the cavity. The FPC couples power into the the gun from a 4 kW RF transmitter and additionally provides for a fine tuning of the resonant frequency. The CsK₂Sb photo-cathode deposited on a molybdenum puck operates at room temperature, while the gun cavity operates at liquid helium temperature of 4 K. The cathodes are inserted into the gun using an ultra-high vacuum (UHV) transport system into a hollow stainless steel cathode stalk, which also serves as a half-wave RF choke with a pick-up antenna located outside of the gun cryostat.

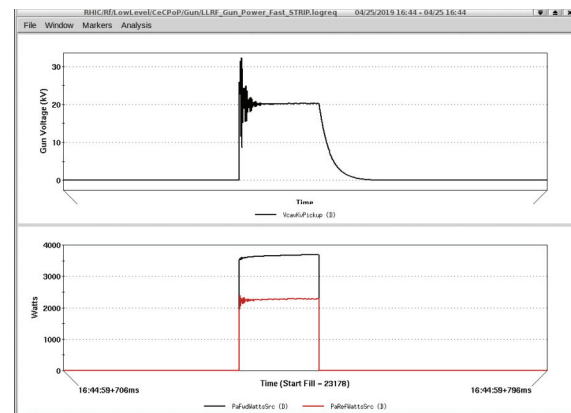


Figure 2: Experimentally observed oscillations of the cavity voltage around the lower MP bound of 20 kV (top plot). The bottom plot shows the pulse of the forward (black) and reflected (red) power, which also demonstrates the oscillations due to the electron avalanche build up.

Even though the gun demonstrated an excellent performance in terms of the delivered beam parameters, the journey towards this achievement was not always flawless. In the beginning of 2017, we observed a significant multipacting (MP) activity in the gun, which was extensively studied experimentally and through numerical simulations [4]. The CW conditioning results for the FPC showed a significant vacuum activity at the gun voltage of about 120 kV, and at the voltages above 300 kV. We also observed a number of low level MP barriers at about 2 kV, 20-27 kV, 30 kV and 40 kV, which corresponded to the build up of the MP electrons in the front rounding of the cavity. An example of a MP event is shown in Fig. 2.

In order to understand the system requirements which would eliminate the MP problem when turning on the gun, we decided to take a different approach, and analyze the com-

combination of the cavity and the FPC in terms of an equivalent circuit.

ANALYTICAL MODEL OF THE MP PASSING

To understand the influence of the coupling between the RF power transmitter and the cavity, we used a standard approach of modeling this interaction as a circuit [5]. The equivalent circuit is shown in Fig. 3.

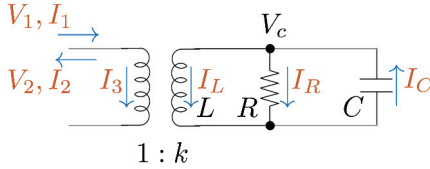


Figure 3: Definition of the currents and voltages in the equivalent circuit of the cavity with a power supply.

Using basic circuit theory one can relate the circuit parameters to the known parameters of an RF cavity. This led us to a system of two self-consistent differential equations, which one needs to solve in order to simulate the process of the cavity start-up: one describing the voltage evolution in a cavity V_c with the presence of a multipactor discharge, and the second one is the equation of exponential growth of the secondary electron avalanche:

$$\begin{cases} \frac{d|V_c|}{dt} = \frac{1}{2\tau} (|V_0| - |V_c|) - f_0 \delta V_{mp} \frac{eN_e(t)}{2Q_0|V_c|} \omega_0 R_{sh}, \\ \frac{dN_e}{dt} = \alpha(|V_c|) N_e. \end{cases} \quad (1)$$

Here V_0 is the maximum achievable voltage of the cavity, which is determined by the available input power and the coupling; τ and $\omega_0 = 2\pi f_0$ are the characteristic time and resonant frequency of a circuit correspondingly. Energy losses due to the MP are determined by the number of the secondary electrons in the MP arc $N_e(t)$, voltage gained by the resonant particles δV_{mp} and the RF parameters of the cavity—shunt impedance R_{sh} and the quality factor Q_0 . α is the rate of the exponential growth of the secondary electrons, and it is related to the secondary emission yield (SEY) and order of multipacting n .

Figure 4 shows the results of simulation for the FPC being inserted half-way in with the maximal available power of 4 kW and SEY coefficient for niobium. As expected, when turning on the cavity, voltage grows linearly with time until it reaches the lower barrier of the MP zone. The number of secondary electrons starts to grow exponentially and the avalanche consumes the input power, which leads to the oscillations of the cavity voltage around the lower MP bound. This process of oscillating voltage around the MP barrier was also observed experimentally (see Fig. 2).

Figure 5 shows a successful passage of the MP events (both 1st and 2nd order) with the maximum coupling and 4 kW available power of the RF transmitter. One can see

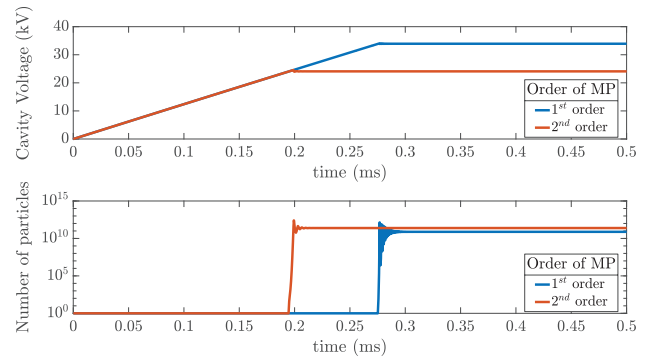


Figure 4: Cavity voltage and the number of secondary electrons as a function of time: 1st and 2nd order MP with the FPC being inserted half-way in, maximal available power of 4 kW, and SEY for Nb.

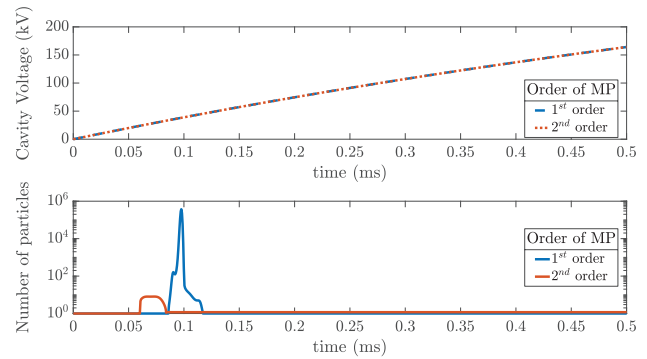


Figure 5: Cavity voltage and the number of secondary electrons as a function of time: 1st and 2nd order MP with the maximum coupling, available power of 4 kW, and adjusted SEY for Nb.

that the growth of the secondary electrons is still present within the cavity body, however, since the position of the FPC is providing the maximum coupling, we cross over the resonant conditions before the electron avalanche can form and bring the cavity down to the MP level.

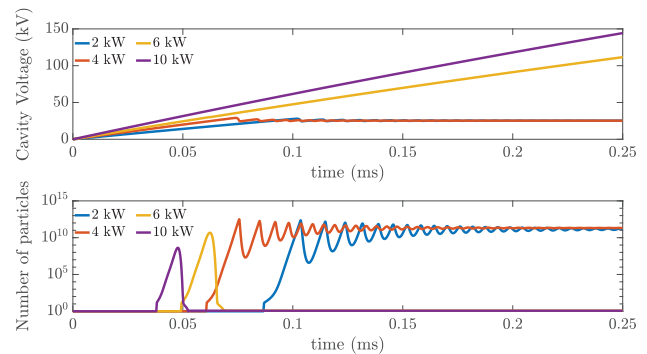


Figure 6: Cavity voltage and the number of secondary electrons as a function of time with the presence of the 2nd order MP: fully inserted FPC, SEY for Nb and various values of the input power.

Figure. 6 and 7 demonstrate the effect of the input power being provided and the scaling of the SEY coefficient on the MP passing.

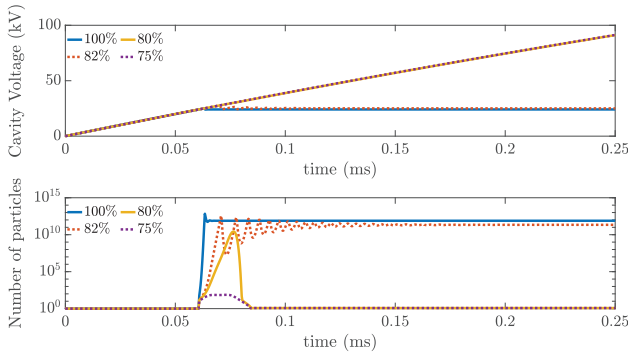


Figure 7: Cavity voltage and the number of secondary electrons as a function of time with the presence of the 2nd order MP: fully inserted FPC, 4 kW input power and different uniform scaling of the SEY for Nb.

EXPERIMENTAL RESULTS

To resolve the MP issue, a system startup script was written in order to lock the gun above the dangerous MP zone as soon as it crossed the threshold. The FPC is first brought to the position of maximal coupling with the cavity, and, with the phase-lock loop (PLL) turned on, the target frequency is checked at a low voltage (~ 1 kV). After setting the threshold, an RF pulse with the full available power ($P_1=4$ kW) was sent in. During the full power pulse, low level RF (LLRF) system monitored the voltage, and as soon as voltage rose above the threshold, the RF power was reduced to $P_2 \sim 500$ W.

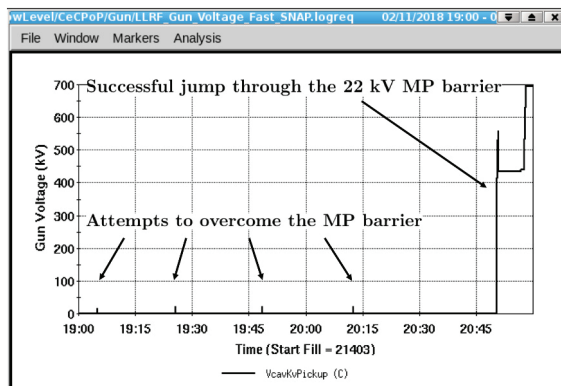


Figure 8: Voltage in the cavity as a function of time demonstrating multiple attempts of passing the MP zones.

Figure 8 demonstrates several attempts at passing the 22 kV barrier: the first 4 spikes show the unsuccessful attempts of bringing the gun to the operational voltage, followed by the successful breakthrough. One can see that after passing the MP threshold of 400 kV, the forward power is lowered and together with the FPC position gradually adjusted to reach the target voltage and frequency.

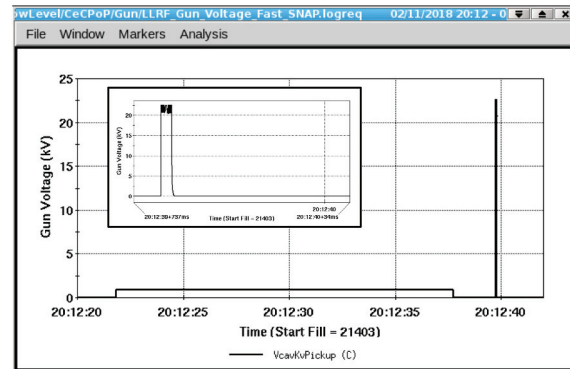


Figure 9: Unsuccessful attempt at passing the 22 kV MP level.

Figure 9 shows the close up of one of the four failed attempts at overcoming the MP barrier from the Fig. 8. The start-up script first sends a 1 kV pulse, allowing the PLL to lock onto the cavity resonance. Once the PLL is locked, the program attempts to reach the threshold voltage. Failure to achieve the target value in 20 ms results in immediate driver turn off.

This procedure allowed us to reach operational gun voltage without tripping on the low level MP.

Overall, performance of the gun was stable throughout the whole commissioning process, being interrupted by rare MP events, which could be easily overcome by turning the gun off for 30 minutes, and bringing it back on using the start-up script. It's important to notice that during the 3 months of operation, the cathode was replaced only once.

CONCLUSION

We presented a simple analytical model which demonstrates the process of overcoming the MP barriers in SRF cavities. We showed, that if treated carefully, SRF photoinjectors with warm photocathodes can successfully operate for months without cathode replacement.

ACKNOWLEDGMENTS

This research used resources of the National Energy Research Scientific Computing Center, which is supported by the Office of Science of the U.S. Department of Energy under Contract No. DE-AC02-05CH11231. Work is supported by Brookhaven Science Associates, LLC under Contract No. DEAC0298CH10886 with the U.S. Department of Energy, DOE NP office grant DE-FOA-0000632, and NSF grant PHY-1415252.

REFERENCES

- [1] V.N. Litvinenko and Ya.S. Derbenev, "Coherent electron cooling", *Phys. Rev. Accel. Beams*, vol. 102, p. 114801, 2009.
- [2] I. Pinayev *et al.*, "Present Status of Coherent Electron Cooling Proof-of-principle Experiment", in *Proc. FEL'14*, Basel, Switzerland, Aug. 2014, paper TUP072, pp. 524–527.

- [3] I. Pinayev *et al.*, “SRF Gun with Warm Photocathode”, presented at the 10th Int. Particle Accelerator Conf. (IPAC’19), Melbourne, Australia, May 2019, paper TUXXP1S1, this conference. 082001, Aug. 2018.
- [4] I. Petrushina *et al.*, “Mitigation of MP in 113 MHz superconducting rf photoinjector”, *Phys. Rev. Accel. Beams*, vol. 21, p. [5] H. Padamsee, J. Knobloch, T. Hays, *RF Superconductivity for accelerators*, John Wiley & Son, 2008.